Co-published by
Institute of Fluid-Flow Machinery
Polish Academy of Sciences
Committee on Thermodynamics and Combustion
Polish Academy of Sciences

Copyright©2024 by the Authors under licence CC BY-NC-ND 4.0

http://www.imp.gda.pl/archives-of-thermodynamics/

Thermal instability of three-dimensional boundary layer stagnation point flow towards a rotating disc

Samir Mamache, Fatsah Mendil*, Faiçal Nait Bouda

Université de Bejaia, Faculté de Technologie, Laboratoire de Mécanique, Matériaux et Energétique (L2ME), 06000 Bejaia, Algeria.
*Corresponding author email: fatsah.mendil@univ-bejaia.dz

Received: 16.01.2024; revised: 19.06.2024; accepted: 19.07.2024

Abstract

In this paper, the thermal instability of a three-dimensional boundary layer axisymmetric stagnation point flow towards a heated horizontal rotating disk is considered. A large number of works have been done on stability analysis. However, they did not check the thermal stability of the non-parallel-flow in the face of small disturbances that occur in the vicinity of the heated rotating disk. The governing equations of the basic flow are reduced to three coupled nonlinear partial differential equations, and solved numerically with the fourth-order Runge-Kutta method. Thermal stability is examined by making use of linear stability theory based on the decomposition of the normal mode of Görtler-Hammerlin. The resulting eigenvalue problem is solved numerically using a pseudo-spectral method based on the expansion of Laguerre's polynomials. The obtained results are discussed in detail through multiple configurations. As the main result, for large Prandtl numbers (Pr), the rotation disk parameter (Ω) has a destabilizing effect while for small Pr (around the unity) it tends to stabilize the basic flow. It was found that as the disk radius $r \to 0$, the flow is linearly stable, and the disturbances grow rapidly away from the stagnation point. For low values of Pr, the flow becomes more stable, and strong thermal gradients are necessary to destabilize it. However, an increase in Pr leads to a significant expansion of the instability region.

Keywords: Thermal instability; Stagnation point; Boundary layer; Rotating disk; Spectral method

Vol. 45(2024), No. 4, 61–72; doi: 10.24425/ather.2024.151997

Cite this manuscript as: Mamache, S., Mendil, F., & Bouda, F.N. (2024). Thermal instability of three-dimensional boundary layer stagnation point flow towards a rotating disc. *Archives of Thermodynamics*, 45(4), 61–72.

1. Introduction

Different phenomena are responsible and act on the transport of matter. The latter can be transported by convection and diffusion as it is encountered in the mixed convection rotating-disk systems. In these processes, all fluids are subjected to a gravitational field in the presence of a thermal gradient that leads spontaneously to variation in the density of the fluid, which gives rise to complex convective movements within the fluid medium [1]. This dynamic behavior can be summarized as being the passage towards a secondary flow leading to the appearance of disturbances that develop within the fluid when viscous and thermal dissipation are overcome by Archimedean thrust. These instabilities, developing in the phenomena of which many applications abound, have benefited from great attention from researchers, scientists, and industrialists in various fields since the Rayleigh-Bernard era, such as gas turbines, rotating-disk air cleaners, medical equipment, etc. This frequently encountered phenomenon is the unique solid film generation process [2] with high performance and great purity. This process depends mainly

Nomenclature

a – positive constant, 1/s
f, h – similarity functions
g – gravitational acceleration, m/s^2
Gr – Grashof number
k – dimensionless wavenumber
L_N – n-th order Laguerre's polynomial
p – dimensionless pressure
P* – pressure, kPa
Pr – Prandtl number
r, z – dimensionless radial and axial coordinates
r*, z* – radial and axial coordinates, m
t – time, s
T – temperature, K
u, v, w – dimensionless velocity components
$\boldsymbol{V}$* – velocity field, m/s
Z_i – location of the collocation node

Greek symbols

α – thermal diffusivity, m^2/s
β – thermal expansion coefficient, 1/K
θ – dimensionless azimuthal coordinate
Θ – dimensionless temperature
υ – kinematic viscosity, m^2/s
ρ – density, kg/m^3
ω – dimensionless temporal growth rate
Ω – dimensionless rotation parameter
Ω* – angular velocity, s^{-1}

Subscripts and Superscripts

c – critical values
N – expansion coefficients vectors in Laguerre's polynomials
w – wall condition
' – differentiation concerning z
* – dimensional quantities
~ – perturbation quantities
^ – complex amplitude functions of perturbations quantities
∞ – free stream condition

Abbreviations and Acronyms

CVD – chemical vapor deposition

on the convection motions linked to interdependent chemical reactions (homogeneous and heterogeneous) in a fluid medium at the heated substrate [3]. Hussain et al. [4] examined the convective traveling modes instability within the boundary layer over a rotating disk in an enforced axial flow under the chemical vapour deposition (CVD) process. In-depth studies of hydrodynamics flow have been motivated by the need to avoid or delay the transition to turbulence in boundary layers. In the case of rotating disk flows, the current field of numerical mechanics requires more advanced techniques for a more precise analysis of these various physical phenomena. In this regard, the first similarity transformations designed to convert the governing partial differential equations into ordinary differential equations were introduced by von Karman [5], who studied with excellence the fluid flow due to the disk rotation. Griffiths [6] introduced von Karman similarity transformations in a generalized Newtonian fluid boundary layer flow due to a rotating disk, after using a high Reynolds number boundary-layer approximation. The corresponding results provided a more accurate description of the flow. Khan et al. [7] analyzed the thermophysical characteristics of liquids and gases near a heated rotating disk. Usman et al. [8] investigated the heat transfer characteristics of a non-isothermal wavy disk rotating in a forced flow. They presented a suitable mechanism for the rapid removal of thermal energy from the surface of the rotating disk. The combination of axisymmetric stagnation flow on a rotating disc was studied by Hannah [9]. Sarkar et al. [10] studied the problem of an axisymmetric oblique stagnation point flow over the rotating disk. Their investigation highlighted that the streamlines shift the location of the stagnation point toward the incoming flow. Forced orthogonal flow with off-center axisymmetric stagnation point flow over a rotating disk was discussed by Wang [11] and Heydari et al. [12].

The instability designates the unstable motion, which refers to small interruptions in laminar flow. These instabilities accumulate and amplify with the presence of thermal and viscous diffusion that occurs within the fluid. When these disturbances develop significantly, the flow is profoundly modified, leading to unstable behaviours under the competition between these effects. An impressive study of this instability phenomenon was presented by Amaouche et al. [13], where they were able to compare the stability characteristics of thermal convection over a non-orthogonal stagnation point flow with those occurring in Hiemenz flow over a heated horizontal plate. Moreover, they examined the presence of a constant magnetic field on the thermal instability of a two-dimensional stagnation point flow, indicating that magnetic fields act to improve its stability [14]. Nait Bouda et al. [15] investigated the effects of mass transfer on the thermal instability of a boundary layer stagnation point flow. Well afterwards, Mendil et al. [16] examined the effect of temperature-dependent viscosity on the thermal instability of two-dimensional stagnation point flow. They found that the intensification of the viscosity of the fluid due to the increase in temperature acts significantly to increase the stability of the flow.

The stability of flows impinging on curved cylindrical surfaces is the subject of several investigations in the literature due to their wide application. This type of convective motion develops a more complex behaviour than flat surfaces. Mittal [17] realized the stabilizing effect as a function of the flow regime on the stability of a flow past a cylinder. The stability of an axisymmetric stagnation flow obliquely striking a circular cylinder in uniform rotation under the effect of the Lorentz force associated with a radial magnetic field has been analyzed by Amaouche et al. [18]. Among the studies on the onset of instabilities of mixed convection over circular cylinders, a two-dimensional boundary layer problem induced by an upward flow on a heated circular horizontal cylinder was investigated by Mouloud et al. [19]. They found that growing instability accumulates in free convection flow and stable sections correspond to forced and mixed convection flow.

Mechanisms having significant effects on flows in most current research are increasingly focused on the complex chal-

lenges encountered in a wide range of current applications. Rotating surfaces with high heat transfer has been the subject of many recent works where investigations are mainly motivated by the possibility of solving the boundary layer equations. At this level, the stability theory aims precisely to prevent the development of disturbances and to determine the critical conditions for the appearance of the instabilities. In this regard, the theoretical and experimental study of linear stability in a spiral vortex in the boundary-layer transition regime on a rotating disk under the effects of streamline curvature and Coriolis force was carried out by Kobayashi et al. [20]. Malik et al. [21] examined the Coriolis effect and the streamline curvature on the stability of three-dimensional rotating disk flow. Lingwood [22] explored the characteristics of boundary layer flow over a rotating disk in an otherwise still fluid by analyzing the inviscid stability of the flow and the stability with viscous curvature, Coriolis and streamlining effects. The instability of trailing-edge flows and wakes is a considerable topic in aerodynamics. Practical interest in this area has driven research to examine the stability of these flows by theoretical and experimental means to improve the understanding of the transition to turbulent flow. In this aspect, an analytic approach for calculating absolutely unstable inviscid modes of the boundary layer on a rotating disk is examined by Türkyılmazoglu and Gajjar [23]. A recent review of the topic relating to the phenomenon of instability of fluid flows can be found in [24,25]. Miller et al. [26] investigated the stability of a heated rotating-disk boundary layer in a temperature-dependent viscosity fluid. Sharma et al. [27] performed a numerical analysis of the nonlinear characteristics of the transition to the chaos caused by thermal instability in a bottom-heated slotted channel undergoing natural convection. Roşca et al. [28] analyzed linear temporal stability of an axisymmetric rotational stagnation flow over a rotating disk under a radially stretching sheet and also presented the radial and azimuthal shear stresses in an axisymmetric rotational stagnation flow. Healey [29] examined the relation between viscous and inviscid absolute instabilities in a boundary layer flow induced by a rotating disk. In some cases, with temperature changes, the viscosity may also undergo a significant change in flow behaviour. Jasmine and Gajjar [30] investigated the absolute and convective instabilities in the incompressible boundary layer on a rotating von Karman disk flow with temperature-dependent viscosity. Wiesche and Helcig [31] investigated experimentally the effect of heating on the stability of the laminar three-dimensional boundary layer flow over a rotating disk. The stability of the three-dimensional boundary layer flow introduced into a rotating disk has been studied numerically using linear stability theory and experimentally by Lee et al. [32]. An overview of developments in the theory of hydrodynamic stability related to the concepts of absolute/convective and local/global instability was performed by Huerre and Monkewitz [33], where they demonstrated how these notions can be used effectively to obtain a description of the spatio-temporal dynamics of open shear flows. Based on the linearized incompressible Navier-Stokes equations, numerical simulations of the flow developing on the surface of a rotating disk were examined with excellence in [34]. Mechanisms having significant effects on flows in most current research are increasingly focused on the complex challenges encountered in a wide range of current applications. Rotating surfaces with high heat transfer has been the subject of many recent works where investigations are mainly motivated by the possibility of solving the boundary layer equations.

In light of these previous findings, even though the above-mentioned studies on instabilities are inherent to many applications, the novelty of this original contribution is focused on the appearance of thermal instability of three-dimensional boundary layer stagnation point flow over a heated rotating disk. For this reason, the thermal instability analysis implemented in [13–16] for two-dimensional flat plate boundary layer flow has been extended and applied to the three-dimensional boundary-layer flow rotating disk. By taking into account the Boussinesq approximation, the resulting dynamic and temperature field are coupled to each other leading to an eigenvalue problem constituted by making use of the linear stability theory. The latter is then solved numerically using the pseudo-spectral collocation method based on Laguerre's polynomials expansion. The rotating disk parameter (Ω) is also one of the novelties or key objectives of this given analysis. Indeed, great attention is given to the competition between rotation parameter and thermal buoyancy forces on the linear stability of the basic flow. Therefore, we seek to examine the evolution of the instability threshold and the effects of pertinent parameters such as the disk radius, the rotating disk parameter, the Prandtl and Grashof numbers (r, Ω, Pr, Gr) linked to the different stages of the transition to turbulence.

2. Model description

2.1. Disk geometry

We consider a heated horizontal disk with a large radius rotating about its axis (z^*) with an angular velocity Ω^* subject to an external axisymmetric orthogonal flow $\boldsymbol{V}_\infty^*(ar^*, 0, -2az^*)$, where a is a positive constant, as shown in Fig. 1. The temperature at the disk (T_w) is assumed to be constant and greater than the external temperature (T_∞). Here, the coordinate frame is not related to the disk rotation.

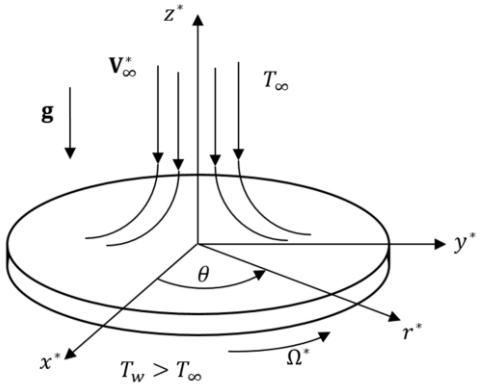

Fig. 1. Physical model and coordinate system for the stagnation point flow considered.

For the steady state, all the physical quantities are assumed to be independent of θ since the flow is axisymmetric about the z^*-axis that is measured from the stagnation point ($r^* = 0$). The physical properties of the fluid are assumed to be constant, except for the density belonging to the buoyancy term given by Boussinesq approximation. We note that in cylindrical coordinates (r^*, θ, z^*), the flow moves within the velocity field u^*, v^* and w^* in the radial, azimuthal and axial directions, respectively. The governing equations of the problem under the assumptions and approximations of the boundary layer are given by [13–16]:

$$\nabla \boldsymbol{V}^* = 0, \tag{1}$$

$$\frac{\partial \boldsymbol{V}^*}{\partial t^*} + (\boldsymbol{V}^* \cdot \nabla)\boldsymbol{V}^* = -\frac{1}{\rho}\nabla P^* + \upsilon \nabla^2 \boldsymbol{V}^* - \boldsymbol{g}\beta(T - T_\infty), \tag{2}$$

$$\frac{\partial T}{\partial t^*} + (\boldsymbol{V}^* \cdot \nabla)T = \alpha \nabla^2 T. \tag{3}$$

The appropriate boundary conditions are applied, such that the radial and azimuthal velocities on the disk are subject to no-slip conditions, while the axial one verifies the non-permeability. Far from the disk, the flow tends to the external stream. Concerning the thermal conditions, the temperature at the disk is maintained at (T_w) whereas, at infinity, the temperature is equal to that of the external flow (T_∞) such as:

$$u^* = 0,\ v^* = r^*\Omega^*,\ w^* = 0,\ T = T_w \ \text{ at } \ z^* = 0, \tag{4}$$

$$u^* = a\, r^*,\ v^* = 0,\ w^* = -2a\, z^*,\ T = T_\infty \ \text{ as } \ z^* \to \infty, \tag{5}$$

where υ designates the kinematic viscosity, ρ is the density of the fluid, $\boldsymbol{g}$ is the gravitational acceleration, β is the thermal expansion coefficient, α is the thermal diffusivity of the fluid and T is the temperature. The dimensionless form of the Eqs. (1)–(3) is obtained by injecting these scaling variables below.

$$t^* = at,\ \ r^* = \sqrt{\upsilon a^{-1}}r,\ \ z^* = \sqrt{\upsilon a^{-1}}z,$$

$$(u^*, v^*, w^*) = \left(\sqrt{\upsilon a}u, \sqrt{\upsilon a}v, \sqrt{\upsilon a}w\right),$$

$$(p^*, T) = (\rho(\upsilon a)p,\ \ \Theta(T_W - T_\infty) + T_\infty).$$

2.2. Solution of the basic flow

In this area, the steady state of the three-dimensional boundary layer flow (Eqs. (1)–(3)) is associated with the cylindrical coordinates r, θ, and z. The buoyancy effect has an important position in the governing differential equations through this mixed convection problem. Taking into account the axial symmetry of the steady state, the equation system is then reduced after neglecting some terms. By subtracting the equation projected along the axial direction from that projected along the radial direction, after deriving them to ($\partial/\partial r$, $\partial/\partial z$) respectively, this leads to eliminating the pressure term in the momentum equation as follows:

$$\frac{\partial}{\partial z}\left(u\frac{\partial u}{\partial r} - \frac{v^2}{r} + w\frac{\partial u}{\partial z}\right) - \frac{\partial}{\partial r}\left(u\frac{\partial w}{\partial r} + w\frac{\partial w}{\partial z}\right) - \mathrm{Gr}\frac{\partial \Theta}{\partial r} = \\ = \frac{\partial}{\partial z}\left(\frac{\partial^2 u}{\partial r^2} + \frac{1}{r}\frac{\partial u}{\partial r} - \frac{u}{r^2} + \frac{\partial^2 u}{\partial z^2}\right) - \frac{\partial}{\partial r}\left(\frac{\partial^2 w}{\partial r^2} + \frac{1}{r}\frac{\partial w}{\partial r} + \frac{\partial^2 w}{\partial z^2}\right), \tag{6}$$

$$u\frac{\partial v}{\partial r} + \frac{uv}{r} + w\frac{\partial v}{\partial z} = \left(\frac{\partial^2 v}{\partial r^2} + \frac{1}{r}\frac{\partial v}{\partial r} - \frac{v}{r^2} + \frac{\partial^2 v}{\partial z^2}\right), \tag{7}$$

$$u\frac{\partial \Theta}{\partial r} + w\frac{\partial \Theta}{\partial z} = \frac{1}{\mathrm{Pr}}\left(\frac{\partial^2 \Theta}{\partial r^2} + \frac{1}{r}\frac{\partial \Theta}{\partial r} + \frac{\partial^2 \Theta}{\partial z^2}\right). \tag{8}$$

The heat transfer is transferred by forced convection, which involves the only normal component of the flow field. Therefore, the temperature field is fully slaved to the normal component of the flow, making the basic flow independent of the Grashof number. Taking into account the following similarity variables [35]:

$$\begin{matrix} u(r,z) = r\, f'(z),\ v(r,z) = r\,\Omega\, h(z), \\ w(r,z) = -2f(z),\ \Theta(r,z) = \Theta(z) \end{matrix}. \tag{9}$$

By subsuming the above similarity transformation (9) in the previous system (Eqs. (6)-(8)), and after some development, the equations are reduced in terms of f, h, Θ, leading to the following ordinary and nonlinear coupled differential equations system:

$$f''' - 2f'^2 + 2ff'' + \Omega^2 h^2 + 1 = 0, \tag{10}$$

$$h'' - 2f'\,h + 2f\,h' = 0, \tag{11}$$

$$\Theta'' + 2\mathrm{Pr} f\Theta' = 0, \tag{12}$$

where the prime (′) denotes differentiation with respect to z, and the transformed boundary conditions are given by:

$$f(0) = f'(0) = 0,\ \ h(0) = 1,\ \ \Theta(0) = 1 \ \ \text{at} \ \ z = 0, \tag{13}$$

$$f'(z) = 1,\ \ h(z) = 0,\ \ \Theta(z) = 0 \ \ \text{as} \ \ z \to \infty. \tag{14}$$

The above equations are, for convenience, formulated in terms of dimensionless variables. The distance along the disk and time are scaled using the factors $\ell = (\upsilon/a)^{1/2}$ and a^{-1}, respectively. Prandtl and Grashof numbers are given, respectively, by $\mathrm{Pr} = \upsilon/\alpha$, $\mathrm{Gr} = \mathrm{g}\beta\,(T_w - T_\infty)\,\ell^3\,/\,\upsilon^2$, and $\Omega = \Omega^*/a$ is the dimensionless rotation parameter. It is preliminary to analyze the basic flow before examining the critical conditions related to the transition to turbulence because the solution of this one appears as variable coefficients in the stability problem. The nonlinear differential Eqs. (10)–(12) with the associated boundary conditions (13) and (14) are solved numerically using the fourth-order Rung-Kutta method with the so-called shooting technique. By keeping an accuracy of 10^{-6}, the process is repeated until the correct results are obtained.

3. Linear stability analysis

The linear stability analysis consists in determining the complex wave numbers and frequencies of the waves that the system supports. In most stability studies, either a purely temporal or spatial instability approach is taken. The limitations of adopting a purely spatial or temporal instability analysis were made clear with the introduction of the concepts of absolute and convective instability. It seems from [22,23,30] that the choice of a temporal or spatial analysis can only be fixed after the behaviour of both the wave number and frequency have been studied in the complex plane and the convective or absolute character of the insta-

bility has been determined. In the problem at hand it is customary to focus attention on temporal instability, i.e. disturbances grow in time at every fixed point in space [19]. In this part, the work is oriented toward the three-dimensional stability analysis in order to examine the temporal growth and spatial amplification of disturbances. Investigations in this section are based on the instability of the flow that occurs after the loss of stability in order to understand the destabilizing mechanisms linked to the different stages of the transition to turbulence. We consider small disturbances propagating along the boundary layer so that the instantaneous quantities can be expressed as the sum of the quantities of the base state and that of the disturbances state as follows:

$$(\bar{u},\bar{v},\bar{w},\bar{p},\bar{\Theta})(r,\theta,z,t) = (u,v,w,p,\Theta)(r,z) + (\tilde{u},\tilde{v},\tilde{w},\tilde{p},\tilde{\Theta})(r,\theta,z,t). \tag{15}$$

By substituting the above decomposition (Eq. (15)) into the Navier-Stokes and energy equations, after subtracting the base state and eliminating the nonlinear terms, we obtain a set of equations governing the evolution of the three-dimensional perturbations in time and space as follows:

$$\left(\frac{\partial}{\partial r}+\frac{1}{r}\right)\tilde{u}+\frac{1}{r}\frac{\partial\tilde{v}}{\partial\theta}+\frac{\partial\tilde{w}}{\partial z}=0, \tag{16}$$

$$\left(\frac{\partial}{\partial t}-\nabla^2+u\frac{\partial}{\partial r}+\frac{v}{r}\frac{\partial}{\partial\theta}+w\frac{\partial}{\partial z}+\frac{\partial u}{\partial r}\right)\tilde{u}-2\frac{v}{r}\tilde{v}+\frac{\partial\tilde{p}}{\partial r}=0, \tag{17}$$

$$\left(\frac{v}{r}+\frac{\partial v}{\partial r}\right)\tilde{u}+\left(\frac{\partial}{\partial t}-\nabla^2+u\frac{\partial}{\partial r}+\frac{v}{r}\frac{\partial}{\partial\theta}+w\frac{\partial}{\partial z}+\frac{u}{r}\right)\tilde{v}+\frac{\partial v}{\partial z}\tilde{w}+\frac{1}{r}\frac{\partial\tilde{p}}{\partial\theta}=0, \tag{18}$$

$$\left(\frac{\partial}{\partial t}-\nabla^2+\frac{v}{r}\frac{\partial}{\partial\theta}+w\frac{\partial}{\partial z}+\frac{\partial w}{\partial z}\right)\tilde{w}+\frac{\partial\tilde{p}}{\partial r}-\mathrm{Gr}\,\tilde{\Theta}=0, \tag{19}$$

$$\left(\frac{\partial}{\partial t}-\frac{1}{\mathrm{Pr}}\nabla^2+\frac{v}{r}\frac{\partial}{\partial\theta}+w\frac{\partial}{\partial z}\right)\tilde{\Theta}+\frac{\partial\Theta}{\partial z}\tilde{w}=0, \tag{20}$$

where ∇^2 refers to the three-dimensional Laplace operator. It should be noted that the quantities (u, v, w, Θ) as previously indicated, represent variable coefficients corresponding to the solution of the basic flow. These coefficients show significant variations in the normal direction (z) and change linearly in the chordwise direction (r), but not in the spanwise direction (θ). The strong dependence of the basic state on radial distance in the problem at hand does not permits the introduction of eigenmodes in the chordwise direction (r), in general. However, the introduction of the eigenmodes in the spanwise (θ) direction to model the problem permits considering the solution separable in the variables θ and t, as discussed previously by Amaouche et al. [14]. Retaining self-similarity for the perturbation amplitude. The disturbance quantities of a general traveling mode can be expressed in the form of the normal mode of Görtler-Hammerlin [36,37], as follows:

$$(\tilde{u},\tilde{v},\tilde{w},\tilde{p},\tilde{\Theta})(r,\theta,z,t) = (r\hat{u},r\hat{v},\hat{w},\hat{p},\hat{\Theta})(z)\exp(ik\theta+\omega t). \tag{21}$$

In the current study, our attention is focused on temporal instability, where the wave number k is real and the temporal growth rate ω is allowed to be complex. Here, $(r\hat{u},r\hat{v},\hat{w},\hat{p},\hat{\Theta})$ are complex amplitude functions of three-dimensional small disturbances. This so-called Görtler-Hammerlin model has been the subject of many works reported before. It was also extended for three-dimensional stability analysis as in [14]. In the present study, we are interested in the region located near the stagnation point, therefore, the non-parallel flow effects of order (r^2) in the terms [$1/r^2$ ($\partial^2V^*/\partial\theta^2$)] are included, and the thermal stability analysis are examined in the concept of non-parallel flow. Introducing the decomposition given by Eq. (21), Eqs. (16)–(20) take the following algebraic system form:

$$2\,\hat{u}+ik\,\hat{v}+D\,\hat{w}=0, \tag{22}$$

$$\left(D^2+2f\,D-2f'-ik\Omega\,h-\frac{k^2}{r^2}\right)\hat{u}+2\left(\Omega\,h-\frac{ik}{r^2}\right)\hat{v}-f''\,\hat{w}=\omega\,\hat{u}, \tag{23}$$

$$-2\left(\Omega\,h-\frac{ik}{r^2}\right)\hat{u}+\left(D^2+2f\,D-2f'-ik\Omega\,h-\frac{k^2}{r^2}\right)\hat{v}-\Omega\,h'\hat{w}-\frac{ik}{r^2}\hat{p}=\omega\,\hat{v}, \tag{24}$$

$$\left(D^2+2f\,D-2f'-ik\,\Omega\,h-\frac{k^2}{r^2}\right)\hat{w}-D\hat{p}+\mathrm{Gr}\hat{\Theta}=\omega\,\hat{w}, \tag{25}$$

$$\left(D^2+2\mathrm{Pr}fD-ik\Omega\mathrm{Pr}h-\frac{k^2}{r^2}\right)\hat{\Theta}-\mathrm{Pr}\,\Theta'\hat{w}=\mathrm{Pr}\omega\,\hat{\Theta}. \tag{26}$$

The disturbances cancel each other out at the wall as well as outside the boundary layer, as indicated by these boundary conditions:

$$\hat{u} = \hat{v} = D\,\hat{w} = \hat{p} = \hat{\Theta} = 0 \quad \text{at} \quad z = 0, \tag{27}$$

$$\hat{u} = \hat{v} = \hat{p} = \hat{\Theta} = 0 \quad \text{as} \quad z \to \infty. \tag{28}$$

The pressure and azimuthal component of the velocity can be deduced from Eqs. (22) and (24) in the form:

$$\hat{v} = -\frac{1}{ik}(\lambda_1 + 2f') - i\,k\,\Omega\,h''(2\hat{u} + D\hat{w}), \tag{29}$$

$$\hat{p} = \frac{r^2}{k^2}(\lambda_1 + 2f') - ik\Omega h''[2(D^2 + 2fD - 2f' - \omega)\hat{u} + (\lambda_1 - 2f' - \omega)D\hat{w} + ik\Omega h'\hat{w}]. \tag{30}$$

The combined Eqs. (22) and (24) lead us to reduce the number of unknowns within the system itself. This simplification is achieved by extracting the term $\hat{v}$ from Eq. (22) and introducing it into Eqs. (23) and (24). Additionally, the pressure $\hat{p}$ is extracted from Eq. (24) and introduced into Eq. (25). Thereafter, we can replace the pressure term as well as the azimuthal velocity component to obtain a reduced system of an eigenvalue problem in the following form:

$$\begin{pmatrix} \lambda_1 - 2f' + 2\xi & \xi D - f'' & 0 \\ \lambda_3 & \lambda_4 & -\frac{k^2}{r^2}\mathrm{Gr} \\ 0 & -\mathrm{Pr}\Theta' & \lambda_5 \end{pmatrix} \begin{pmatrix} \hat{u} \\ \hat{w} \\ \hat{\theta} \end{pmatrix} = \omega \begin{pmatrix} 1 & 0 & 0 \\ 2D & \lambda_2 & 0 \\ 0 & 0 & \mathrm{Pr} \end{pmatrix} \begin{pmatrix} \hat{u} \\ \hat{w} \\ \hat{\theta} \end{pmatrix}, \tag{31}$$

such as

$$D = \frac{\partial}{\partial z}, \quad \lambda_1 = (\lambda_2 + 2fD - i\,k\,\Omega\,h), \quad \lambda_2 = D^2 - \frac{k^2}{r^2}, \quad \xi = \frac{2}{k^2}\left(i\,k\,\Omega\,h + \frac{k^2}{r^2}\right),$$

$$\lambda_3 = 2(D^2 + 2f\,D)D - 4f'', \quad \lambda_4 = \lambda_1 D^2 - 2f''\,D - \left[\frac{k^2}{r^2}(\lambda_1 + 2f') - ik\Omega h''\right],$$

$$\lambda_5 = \lambda_2 + 2\mathrm{Pr}fD - i\,k\,\mathrm{Pr}\,\Omega\,h.$$

This combination will not only facilitate the numerical solution of the system but also minimize the computation time.

4. Computational method

The basic flow is solved simultaneously with the stability problem, which appears in the form of variable coefficients. To approximate the solution of the problem, the flow stability characteristics are calculated by solving the generalized algebraic eigenvalue problem (31) through a pseudo-spectral method based on the expansion of Laguerre's polynomials. The most important feature of this method is exponential convergence, which allows high precision with a modest number of collocation points. However, the use of Laguerre polynomials is motivated by the distribution of their zeros, i.e. the first zeros are close to each other and this distribution is perfectly suited to describe regions of strong gradients in the boundary layers. According to mathematical models, an approach of the three-dimensional complex amplitude functions is given as an approximation in the form $\hat{\phi}_N(\hat{u}_N, \hat{w}_N, \hat{\Theta}_N)$ [13–16], defined as:

$$\hat{\phi}_N(z) = \exp(-z)\sum_{i=1}^{N} \frac{zL_N(z)}{z_i(z-z_i)\frac{dL_N(z_i)}{dz}}\phi_N(z_i). \tag{32}$$

The simplification related to this approximation gives rise to an algebraic eigenvalue system in terms of discretized square matrices ($3\times N$, $3\times N$) such as:

$$\begin{pmatrix} \boldsymbol{\lambda}_1 - 2\boldsymbol{f}' + 2\boldsymbol{\xi} & \boldsymbol{\xi}(\mathbf{D} - \mathbf{I}) - \boldsymbol{f}'' & \mathbf{0} \\ \boldsymbol{\lambda}_3 & \boldsymbol{\lambda}_4 & -\frac{k^2}{r^2}\mathrm{Gr}\mathbf{I} \\ \mathbf{0} & -\mathrm{Pr}\boldsymbol{\Theta}' & \boldsymbol{\lambda}_5 \end{pmatrix} \begin{pmatrix} \hat{\boldsymbol{u}}_N \\ \hat{\boldsymbol{w}}_N \\ \hat{\boldsymbol{\theta}}_N \end{pmatrix} = \omega \begin{pmatrix} \mathbf{I} & \mathbf{0} & \mathbf{0} \\ 2(\mathbf{D} - \mathbf{I}) & \boldsymbol{\lambda}_2 & \mathbf{0} \\ \mathbf{0} & \mathbf{0} & \mathrm{Pr}\mathbf{I} \end{pmatrix} \begin{pmatrix} \hat{\boldsymbol{u}}_N \\ \hat{\boldsymbol{w}}_N \\ \hat{\boldsymbol{\theta}}_N \end{pmatrix}, \tag{33}$$

such as

$$\boldsymbol{\lambda_1} = (\boldsymbol{\lambda_2} + 2\boldsymbol{f}\mathbf{D} - 2\boldsymbol{f} - ik\Omega\boldsymbol{h}), \qquad \boldsymbol{\lambda_2} = \mathbf{D}^2 - 2\mathbf{D} + \left(1 - \frac{k^2}{r^2}\right)\boldsymbol{I}, \quad \boldsymbol{\xi} = \frac{2}{k^2}\left(ik\Omega\boldsymbol{h} + \frac{k^2}{r^2}\mathbf{I}\right),$$

$$\boldsymbol{\lambda_3} = 2(\mathbf{D}^2 + 2(\boldsymbol{f} - \mathbf{I})\mathbf{D} + \mathbf{I})(\mathbf{D} - \mathbf{I}) - 4\boldsymbol{f}'',$$

$$\boldsymbol{\lambda_4} = \boldsymbol{\lambda_1}(\mathbf{D}^2 - 2\mathbf{D} + \mathbf{I}) - 2\boldsymbol{f}''(\mathbf{D} - \mathbf{I}) - \left(\frac{k^2}{r^2}(\boldsymbol{\lambda_1} + 2\boldsymbol{f}') - ik\Omega\boldsymbol{h}''\right),$$

$$\boldsymbol{\lambda_5} = \boldsymbol{\lambda_2} + 2\mathrm{Pr}\boldsymbol{f}(\mathbf{D} - \mathbf{I}) - ik\,Pr\,\Omega\,\boldsymbol{h}.$$

The square matrices **D** and **I** are the matrices associated with the differential operator *D* and the identity matrix, respectively. Parameters $\widehat{\boldsymbol{u}}_N, \widehat{\boldsymbol{w}}_N$ and $\widehat{\boldsymbol{\theta}}_N$ denote the expansion coefficients vector. The system (33) can be expressed in terms of square matrices **A** and **B** taking the form $(\mathbf{A} - \omega\mathbf{B})\,\widehat{\boldsymbol{\phi}}_N$. For that, the matrix system does not have a unique solution; the matrix $\mathbf{A} - \omega\,\mathbf{B}$ must be regular to have non-trivial solutions. The combination of the parameters *r*, Ω, Pr, and Gr allows us to examine the critical conditions for the appearance of instability which occurs for the minimum value of Gr that cancels the det(**A**) at marginality.

5. Results and discussion

5.1. Basic flow

Within the framework of this study, the instability of the three-dimensional stagnation point flow is examined in cylindrical coordinates. The solution of the basic flow appears as variable coefficients in the generalized algebraic eigenvalue problem (33). Parameters *f*, *h*, and Θ are some of the dominating parameters controlling the stability problem, which must be examined at the beginning.

The governing basic flow (Eqs. (10)–(12)) subject to the boundary conditions (13)–(14) is reduced using the shooting technique method, which consists of converting it into a set of first-order differential equations to facilitate its resolution. With the prescribed values of Pr and Ω, the primary solution of the basic flow (1)–(3) is first obtained numerically by the iterative fourth-order Runge-Kutta method. For a step of 10^{-6}, the calculations proved sufficiently accurate. The resolution of the equations was carried out from $z = 0$ to $z \to \infty$ under Dirichlet boundary conditions imposed on the considered problem. The numerical scheme can be optimized by reducing the step size $\Delta z = 0.001$ in the considered range [0,10]. However, for such high levels of precision, the iteration process requires a significant increase in computation time. The validation is carried out by a calculation code where the results of $f''(0)$ and $h'(0)$ are reported in Tables 1 and 2. For all given values of the rotation parameter Ω, the results show considerable agreement with respect to those reported in [10–12]. Table 3 gives computa-tional results of the effects of rotation parameter and Prandtl number on the rate of heat transfer, indicating that an increase in both parameters leads to the increase in the rate of heat transfer. Numerical calculations are carried out for Ω and Pr ranging from 0 to 10 and 0.7 to 7, respectively. Using the numerical procedures described above, the radial, azimuthal velocity and temperature distributions for the flow considered from Eqs. (10)–(12) are displayed in Fig. 2.

Table 1. Initial values of f'' for various values of Ω.

	$f''(0)$			
Ω	**Present work**	**Sarkar [10]**	**Wang [11]**	**Heydari [12]**
0	1.311938	1.31194	1.31194	1.311958
1	1.573923	1.57392	1.57539	1.573930
2	2.295649	2.29564	2.2951	2.295639
5	6.259882	6.25987	6.2602	6.259869
7	9.916523	9.91652	9.9165	9.916513

Table 2. Initial values of h' for various values of Ω.

	$h'(0)$			
Ω	**Present work**	**Sarkar [10]**	**Wang [11]**	**Heydari [12]**
0	-1.074667	-1.07467	-1.07467	-1.074697
0.5	-1.083905	–	-1.0839	-1.083934
1	-1.109996	-1.11000	-1.1100	-1.110020
2	-1.196826	-1.19676	-1.1968	-1.196841
5	-1.531978	-1.53198	-1.5320	-1.531983
7	-1.745103	-1.74511	-1.7451	-1.745106

Table 3. Initial values of $-\Theta'(0)$ for various values of Ω and Pr

	$-\Theta'(0)$	
Ω	**Pr = 0.7**	**Pr = 7**
0	0.6654	1.5458
0.5	0.6696	1.5620
1	0.6817	1.6078

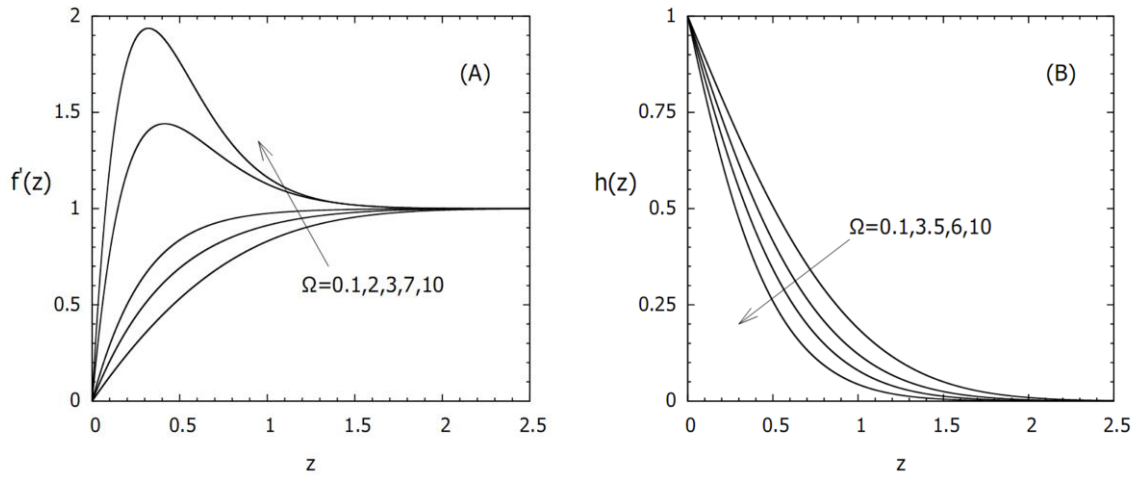

Fig. 2. Variation of $f'(z)$ and $h(z)$ for different values of Ω and Pr = 7.

Figure 2 shows the variation in velocity field $f'(z)$ and $h(z)$ functions for different values of the rotation parameter. As **Ω** is increased, the radial velocity profile increases near the stagnation point flow. When **Ω** is greater than 3.33, it is observed that with increased **Ω**, the rotation effect generates an overshoot of the radial velocity. The influence of the rotation parameter on the $h(z)$ component is presented in Fig. 2B. It can be seen that an increase in **Ω** generates a gradual decrease in the azimuthal velocity.

The results presented in Fig. 3 confirm those obtained in previous studies [14,15] indicating that the temperature of the fluid reduces for large Prandtl numbers, because with an increase in Pr the thermal diffusivity decreases. The fluid particles are able to conduct less heat and consequently temperature profiles decrease with a reduction in thermal boundary-layer thickness. In this case, temperature profiles within the fluid will be strongly influenced by the velocity profiles.

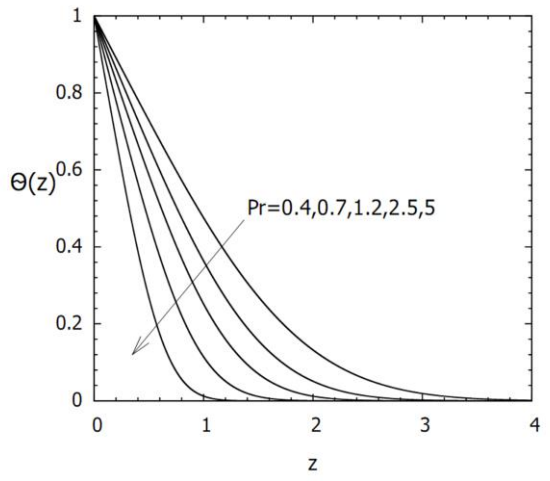

Fig. 3. Temperature profile change for a wide range of Prandtl numbers and Ω = 1.

5.2. Stability analysis

The generalized algebraic eigenvalue problem given by Eq. (33) has been solved numerically using a pseudo-spectral method based on the expansion of Laguerre's polynomials. Numerical computations are performed for several values of control parameters such as Prandtl number (Pr), disk radius (r) and rotation parameter (**Ω**). The neutral curve is generated using Newton's method where the iteration process is repeated until $|\det(\mathbf{A})|$ vanishes with the assumed tolerance $|\det(\mathbf{A})| \leq 10^{-6}$. For satisfactory convergence, the effect of the level of truncation N was taken into account on the critical conditions for the onset of instability. Convergence criteria are based on the relative difference of $|Gr_{c,i+1}-Gr_{c,i}|$. This showed that the accuracy of the numerical scheme can be improved by increasing the number of collocation nodes.

Figure 4 shows the effect of the number of collocation nodes N on the critical Grashof error. It can be clearly seen that the number of polynomials required rises by increasing the Pr number. This can be explained by the fact that an increase in Pr reduces the thermal boundary layer thickness, which requires

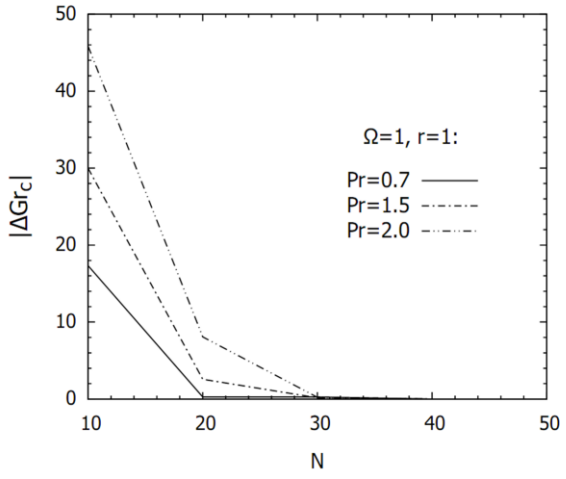

Fig. 4. Effect of the number of collocation nodes N on the critical Grashof error.

a larger number of terms in order to avoid spurious nodes and preserve the prescribed precision.

The stability analysis depicts that the critical conditions of the onset of thermal instability are significantly affected by disk rotation. Generally, one can observe that the disk radius (r), rotation parameter (Ω) and Prandtl number (Pr) act to increase or decrease the stability of the flow. An overview of the stability properties of the basic flow can be seen from the sequence of neutral stability curves displayed in Fig. 5. We recall that each curve illustrates a minimum value (critical) of the Grashof number (Gr_c) for which the boundary layer is stable or unstable. The unstable state lies above the curve, while the opposite behaviour lies below it. As it can be seen from Fig. 5A, for typical values of the rotation parameter, an increase in Ω leads to a decrease in Gr_c. Therefore, increasing Ω acts to destabilize the basic flow (i.e. Gr_c decreases and the unstable regions are expanding). This can be explained by the fact that the induced centrifugal forces by increasing Ω tend to destabilize the basic flow as previously observed in Fig. 2. In Fig. 5B, the sensitivity of the base flow to small disturbances at various locations along the disk radius (r) is examined to distinguish between the most stable and the least stable positions. For the given values of r, the corresponding neutral stability curves show that as we approach the stagnation point, the Gr_c increases and the unstable modes become imperceptible as $r \to 0$. In this region, the flow

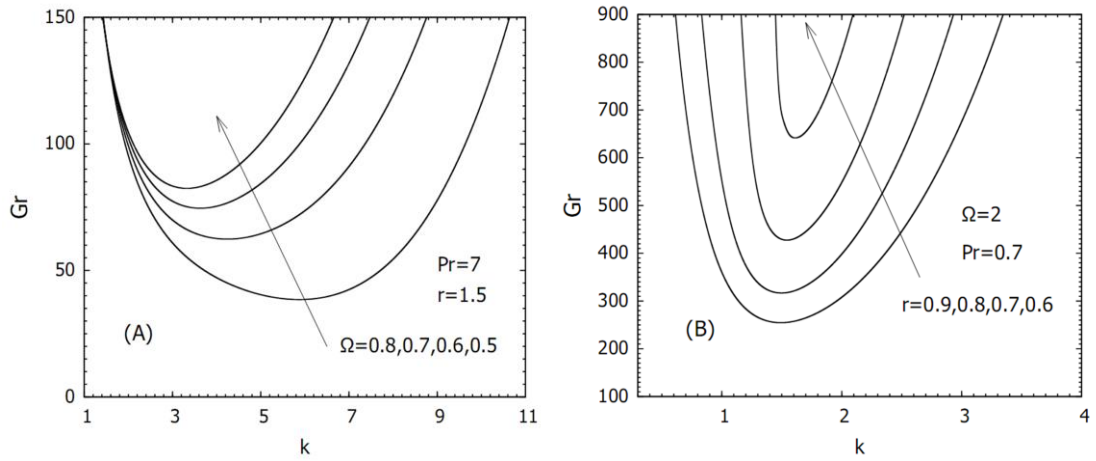

Fig. 5. Neutral stability curves for different values of: A) rotation parameter Ω, B) disk radius r.

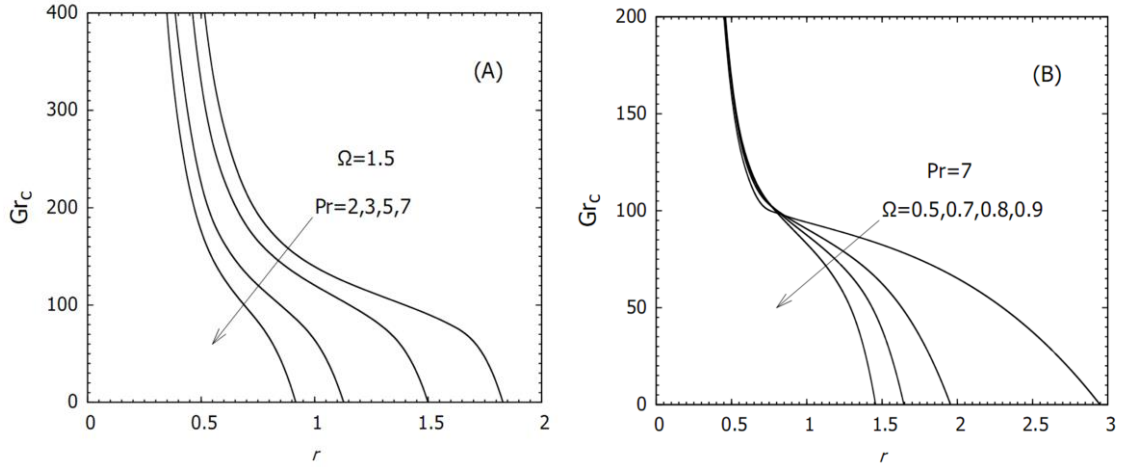

Fig. 6. Critical Grashof number as a function of the disk radius: A) for different values of Pr, B) with varying Ω.

remains more stable. In the opposite case, away from the stagnation point ($r \to \infty$), Gr_c becomes very weak and the flow becomes unstable even without heating effect.

To distinguish between stable and unstable regions along the disk radius, the results discussed in Fig. 5 can be interpreted in another aspect to check their validity. It is found that the same observation has been confirmed again. Figure 6 provides an overview of the critical Grashof number (Gr_c) as functions of the disk radius (r) for different values of Prandtl number and rotation parameter (Ω). We can see that Gr_c grows rapidly to infinity when $r \to 0$ (by approaching the stagnation point). However, the variation of Gr_c becomes significantly weaker and decreases

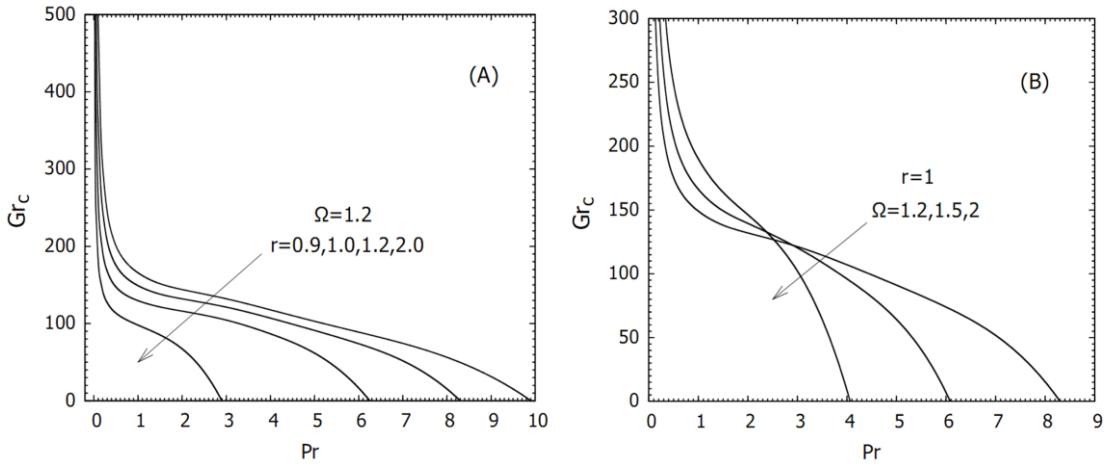

Fig. 7. Critical Grashof number (Gr_c) as a function of Pr: A) for different values of disk radius (r), B) for different values of rotation parameter (Ω).

rapidly moving away from the stagnation point. The observations show that disturbances decrease as one approaches the stagnation point (at the vicinity of the stagnation point the flow remains stable) and increase significantly as one moves away from it as shown previously in Fig. 5B. For large values of r (far away from the stagnation point), the critical Grashof number can reach zero values and the flow becomes unstable even without the thermal effects. As well, the transition to a secondary flow is linked to viscous instability.

More precisely, instability refers to the transition to a secondary flow, which occurs at a certain critical Grashof number. This transition can be explained by the influence of the buoyancy forces term in Eq. (19). The above results shown in the (k, Gr) plane indicated that the most unstable branches effectively correspond to large values of rotation parameter and disk radius. However, strong thermal gradients notably produce an opposite effect, i.e. small values of Pr are reflected with an attenuation of the instability region.

Regarding the critical conditions for the appearance of instability. Figure 7 shows an overall overview of the evolution of the critical Grashof number (Gr_c) as function of Pr. For a given values of r and Ω, both figures show that Gr_c grows very rapidly when $Pr \to 0$, i.e. a small change in the Pr affects significantly the stability threshold. However, when $Pr \to \infty$ then Gr_c becomes insensitive to Pr and decreases suddenly with a large expansion of instability region as observed previously by Amaouche et al. [13]. This can be explained by the fact that, for low values of Pr, the thermal disturbances are promoted to be dissipated rapidly, and the variation in Gr_c number corresponding to the most unstable mode remains imperceptible [15]. This means that larger thermal gradients are required to destabilize the basic flow. In contrast, for larger Prandtl numbers, thermal dissipation is slower and the thermal fields are predominated by the velocity fields, which make the equilibrium less stable. Also, the corresponding thermal boundary-layer thickness is weak, which promotes instability even close to the stagnation point. Concerning the rotation parameter, its influence on the stability of the basic flow changes for small and great Pr. For large Pr, Ω has a destabilizing effect while for small Pr (around the unity) it tends to stabilize the basic flow.

The description of the physical mechanism governing this phenomenon was also carried out by establishing a concept to justify the occurrence of these fluctuations on the least stable and the most unstable branches. Figure 8 shows the temporal

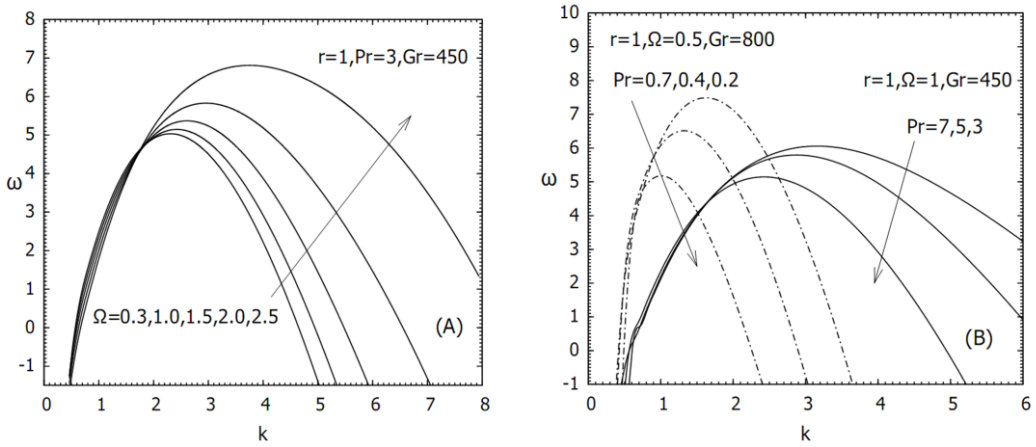

Fig. 8. Temporal growth rate as a function of wavenumber k for different values of Ω and Pr.

growth rate (ω) versus the wavenumber (k) for different values of Pr and Ω. Knowing that the stable region corresponds to negative values of temporal growth rate ($\omega < 0$), while the unstable region corresponds to positive ones ($\omega > 0$). At $r = 1$ and Gr = 450 and 800, it is seen from both figures that an increase in the Prandtl number and rotation parameter leads to a progressive expansion of the most unstable modes. However, the results indicate that the heating effect significantly increases the stability of the base flow, i.e. the most stable modes are improving as the Prandtl number decreases ($Pr \rightarrow 0$) [19]. The graphs confirm that the effect of heating increases the stability of the flow while the effect of disk rotation decreases its stability. Within a specific range of the control parameters, the results also seem to confirm the stability analysis shown in Fig. 5.

6. Conclusions

In this paper, the thermal instability characteristics of three-dimensional stagnation point flow over a heated rotating disk is carried out under the effect of heat transfer, rotation parameter and disk radius. The eigenvalue problem governing the stability process has been constituted by applying linear stability theory, and solved numerically by making use of a pseudo-spectral method using Laguerre's polynomials. Our findings provide a significant contribution by examining the evolution of thermal instabilities in the boundary layer stagnation point flow under the appropriate control parameters, and the main results presented in this study can be summarized as follows:

i) Thermal excitation generates three-dimensional instabilities in the presence of heat transfer, which leads to a large critical Grashof number for the onset of instability.
ii) An increase in fluid temperature gives a larger critical Grashof number for the onset of thermal instability. In addition, for quite small values of the Prandtl number, the flow tends to be in a stable state.
iii) Expansion of unstable regions far from the stagnation point ($r \rightarrow \infty$), and the opposite effect turns out to be observed as we approach it ($r \rightarrow 0$). This region appears to be the most stable area with a very high critical Grashof number.
iv) The rotation parameter presents a destabilizing effect leading to the expansion of instability regions.

In perspective, the work can be improved by investigating the spatio-temporal instabilities analysis in order to identify possible convective/absolute and local/global instabilities. In addition, the asymptotic analysis of the instability can be studied and it is of capital importance to further enhance the validity of the stable and unstable regimes.

References

[1] Shevchuk, I.V. (2009). *Convective Heat and Mass Transfer in Rotating Disk Systems*. Springer, Berlin - Heidelberg. doi: 10.1007/978-3-642-00718-7

[2] Evans, G., & Greif, R. (1987). A numerical model of the flow and heat transfer in a rotating disk chemical vapor deposition reactor. *Journal of Heat Transfer*, 109(4), 928–935. doi: 10.1115/ 1.3248205

[3] Evans, G.H., & Greif, R. (1988). Forced flow near a heated rotating disk: A similarity solution. *Numerical Heat Transfer*, 14(3), 373–387. doi: 10.1080/10407788808913650

[4] Hussain, Z., Garrett, S.J., & Stephen, S.O. (2011). The instability of the boundary layer over a disk rotating in an enforced axial flow. *Physics of Fluids*, 23, 114108. doi: 10.1063/ 1.3662133.

[5] Kármán, Th.V. (1921). Über laminare und turbulente Reibung. ZAMM – *Journal of Applied Mathematics and Mechanics*, 1(4), 233–252 (in German). doi: 10.1002/zamm.19210010401

[6] Griffiths, P.T. (2015). Flow of a generalised Newtonian fluid due to a rotating disk. *Journal of Non-Newtonian Fluid Mechanics*, 221, 9–17. doi: 10.1016/j.jnnfm.2015.03.008

[7] Khan, M., Salahuddin, T., & Stephen, S.O. (2020). Thermo-physical characteristics of liquids and gases near a rotating disk. *Chaos Solitons & Fractals*, 141, 110304. doi: 10.1016/j.chaos. 2020.110304

[8] Usman, M., Mehmood, A., & Weigand, B. (2020). Heat transfer from a non-isothermal rotating rough disk subjected to forced flow. *International Communication in Heat and Mass Transfer*, 110, 104395. doi:10.1016/j.icheatmasstransfer.2019. 104395

[9] Hannah, D.M. (1947). Forced flow against a rotating disc. *British Aeronautical Research Council Reports & Memoranda*, 2772.

[10] Sarkar, S., & Sahoo, B. (2021). Oblique stagnation flow towards a rotating disc. *European Journal of Mechanics - B/Fluids*, 85, 82–89. doi: 10.1016/j.euromechflu.2020.08.009

[11] Wang, C.Y. (2008). Off-centered stagnation flow towards a rotating disc. *International Journal of Engineering Science*, 46(4), 391–396. doi: 10.1016/j.ijengsci.2008.01.014

[12] Heydari, M., Loghmani, G.B., Rashidi, M.M., & Hosseini, S.M. (2015). A numerical study for off-centered stagnation flow towards a rotating disc. *Propulsion and Power Research*, 4(3), 169–178. doi: 10.1016/j.jppr.2015.07.004

[13] Amaouche, M., & Boukari, D. (2003). Influence of thermal convection on non-orthogonal stagnation point flow. *International Journal of Thermal Sciences*, 42(3), 303–310. doi: 10.1016/ S1290-0729(02)00031-5

[14] Amaouche, M., Naït-Bouda, F., & Sadat, H. (2005). The onset of thermal instability of a two-dimensional hydromagnetic stagnation point flow. *International Journal of Heat and Mass Transfer*, 48(21-22), 4435–4445. doi:10.1016/j.ijheatmasstransfer.2005. 05.003

[15] Naït Bouda, F., Mendil, F., Sadaoui, D., Mansouri, K., & Amaouche, M. (2015). Instability of opposing double diffusive convection in 2D boundary layer sta gnation point flow. *International Journal of Thermal Sciences*, 98, 192–201. doi: 10.1016/ j.ijthermalsci.2015.07.014

[16] Mendil, F., Naït-Bouda, F., & Sadaoui, D. (2015). Effect of temperature dependent viscosity on the thermal instability of two-dimensional stagnation point flow. *Mechanics & Industry*, 16, 506. doi: 10.1051/meca/2015031

[17] Mittal, S. (2010). Stability of flow past a cylinder: Energy budget of eigenmodes. *International Journal for Numerical Methods in Fluids*, 63, 533–547. doi: 10.1002/fld.2084

[18] Amaouche, M., Naït-Bouda, F., & Sadat, H. (2007). Oblique axisymmetric stagnation flows in magnetohydrodynamics. *Physics of Fluids*, 19, 114106. doi: 10.1063/1.2804957

[19] Mouloud, S., Nait-Bouda, F., Sadaoui, D., & Mendil F. (2019). The onset of instabilities in mixed convection boundary layer flow over a heated horizontal circular cylinder. *Journal of Thermal Science and Engineering Applications*, 11(5), 51002. doi: 10.1115/1.4042586

[20] Kobayashi, R., Kohama, Y., & Takamadate, Ch. (1980). Spiral vortices in boundary layer transition regime on a rotating disk. *Acta Mechanica*, 35, 71–82. doi: 10.1007/BF01190058

[21] Malik, M.R., Wilkinson, S.P., & Orszag, S.A. (1981). Instability and transition in rotating disk flow. *American Institute of Aeronautics and Astronautics*, 19(9), 1131–1138. doi: 10.2514/ 3.7849

[22] Lingwood, R.J. (1995). Absolute instability of the boundary layer on a rotating disk. *Journal of Fluid Mechanics*, 299, 17–33. doi: 10.1017/S0022112095003405

[23] Turkyilmazoglu, M., & Gajjar, S.J.B. (2001). An analytic approach for calculating absolutely unstable inviscid modes of the boundary layer on a rotating disk. *Studies in Applied Mathematics*, 106(4), 419–435. doi.org/10.1111/1467-9590. 001733

[24] Turkyilmazoglu, M. (2019). Direct contact melting due to a permeable rotating disk. *Physics of Fluids*, 31, 023603. doi: 10.1063/1.5086724

[25] Turkyilmazoglu, M. (2010). Heat and mass transfer on the MHD fluid flow due to a porous rotating disk with hall current and variable properties. *Journal of Heat and Mass Transfer*, 133(2), 021701. doi: 10.1115/1.4002634

[26] Miller, R., Griffiths, P., Hussain, Z., & Garrett, S.J. (2020). On the stability of a heated rotating-disk boundary layer in a temperature-dependent viscosity fluid. *Physics of Fluids*, 32, 024105. doi: 10.1063/1.5129220

[27] Sharma, A., Mahapatra, P.S., Manna, N.K., Ghosh, K., Wahi, P., & Mukhopadhyay, A. (2016). Thermal instability-driven multiple solutions in a grooved channel. *Numerical Heat Transfer, Part A: Applications*, 70(7), 776–790. doi: 10.1080/ 10407782. 2016.1192936

[28] Roşca, N.C., & Pop, I. (2017). Axisymmetric rotational stagnation point flow impinging radially a permeable stretching/shrinking surface in a nanofluid using Tiwari and Das model. *Scientific Reports*, 7, 40299. doi: 10.1038/srep40299

[29] Healey, J.J. (2004). On the relation between the viscous and inviscid absolute instabilities of the rotating-disk boundary layer. *Journal of Fluid Mechanics*, 511, 179–199. doi: 10.1017/ S0022112004009565

[30] Jasmine, H.A., & Gajjar, J.S.B. (2005). Absolute and convective instabilities in the incompressible boundary layer on a rotating disk with temperature-dependent viscosity. *International Journal of Heat and Mass Transfer*, 48(5), 1022–1037. doi: 10.1016/ j.ijheatmasstransfer.2004.07.036

[31] Wiesche, S., & Helcig, C. (2022). Effect of heating on the stability of the three-dimensional boundary layer flow over a rotating disk. *E3S Web of Conferences*, 345, 02007. doi: 10.1051/ e3sconf/202234502007

[32] Lee, Y.-Y., Hwang, Y.-K., & Lee, K.-W. (2003). The flow instability over the infinite rotating disk. *KSME International Journal*, 17(9), 1388–1395. doi: 10.1007/BF02982480

[33] Huerre, P., & Monkewitz, P.A. (1990). Local and global instabilities in spatially developing flows. *Annual Review of Fluid Mechanics*, 22, 473–537. doi: 10.1146/annurev.fl.22.010190. 002353

[34] Appelquist, E., Schlatter, P., Alfredsson, P.H., & Lingwood, R.J. (2015). Global linear instability of the rotating-disk flow investigated through simulations. *Journal of Fluid Mechanics, 765*, 612–631. doi: 10.1017/jfm.2015.2

[35] Mustafa, M. (2017). MHD nanofluid flow over a rotating disk with prtial slip effects: Buongiorno-model. *International Journal of Heat and Mass Transfer*, 108(B), 1910–1916. doi: 10.1016/ j.ijheatmasstransfer.2017.01.064

[36] Görtler, H. (1955). Dreidimensionale Instabilität der ebenen Staupunktströmung gegenüber wirbelartigen Störungen. In *50 Jahre Grenzschichtforschung*, H. Görtler, W. Tollmein (Eds.), (pp. 304–314), Vieweg und Teubner Verlag, Wiesbaden (in German). doi: 10.1007/978-3-663-20219-6_30

[37] Hämmerlin, G. (1955). Zur Instabilitätstheorie der ebenen Staupunktströmung. In *50 Jahre Grenzschichtforschung*, H. Görtler, W. Tollmein (Eds.), (pp. 315–327), Vieweg und Teubner Verlag, Wiesbaden (in German). doi: 10.1007/978-3-663-20219-6_31.